HIGH-SPATIAL-RESOLUTION OH AND CH_2O PLIF VISUALIZATION IN A DUAL-MODE SCRAMJET COMBUSTOR

Clayton M. Geipel

Department of Mechanical and Aerospace Engineering, University of Virginia

Abstract

A high-spatial-resolution planar laser-induced fluorescence (PLIF) imaging system was constructed and used to image a cavity-stabilized, premixed ethylene-air flame. The flame was created within a continuous flow, electrically-heated supersonic combustion facility consisting of a Mach 2 nozzle, an isolator with flush-wall fuel injectors, a combustor with a cavity flameholder of height 9 mm and optical access, and an extender. Tests were conducted at total temperature 1200 K, total pressure 300 kPa, equivalence ratio near 0.4 in the combustor, and Mach number near 0.6 in the combustor. A frequency-doubled Nd:YAG laser pumped a dye laser, which produced light at 283.55 nm. The beam was shaped into a light sheet with full width half-maximum 25 μm, which illuminated a streamwise plane that bisected the cavity. An intensified camera system imaged OH in this plane with a square 6.67 mm field of view and in-plane resolution 39 μm. Images were taken between the backward-facing step and 120 mm downstream of the step. OH structures as small as 110 μm were observed. CH_2O was excited using 352.48 nm light; the smallest observed CH_2O structures were approximately 200 μm wide. Approximately 15,000 images per species were processed and used to compute composite images.

Introduction

High-resolution OH and CH_2O PLIF imaging was performed at the University of Virginia Supersonic Combustion Facility (UVaSCF) on a premixed ethylene-air flame that was anchored and stabilized by a cavity flameholder. UVaSCF is a continuous-flow, electrically-heated, clean-air ground test facility with optical access that produces an enthalpy simulating a Mach $M = 5$ scramjet flight. This work corresponds to UVaSCF "modified Configuration E":[1] a $M = 2$ nozzle followed by an isolator with fuel injectors, a combustor test section, and an outlet. Tests were performed with total temperature 1200 K, total pressure 300 kPa, local equivalence ratios near 0.4, and $M = 0.6$ at the combustor.

Nonintrusive optical diagnostic techniques such as planar laser-induced fluorescence (PLIF) are often used to characterize turbulent flame structures.[2] PLIF is a technique in which a cylindrical lens expands a circular laser beam in a given direction and then a spherical lens collimates the beam in the given direction and focuses it in the orthogonal direction, creating a thin sheet of laser light. The wavelength of this sheet is tuned to match an absorption band of a chemical species of interest, usually an intermediate product of combustion. The species emits broadband fluorescence, which is captured by an intensified camera. This provides an instantaneous, planar map of qualitative or quantitative concentration measurements. PLIF images can be compared to computational species concentration results in order to refine computational and theoretical models.

Previous studies have imaged OH[3] and CH_2O[4] at UVaSCF; the current work presents data at a higher spatial resolution, resolving smaller flame structures. The resolution of

PLIF images depends on both the resolution of the imaging and camera system and on the laser sheet thickness. Turbulent flows are highly three-dimensional, and PLIF signal is integrated over the sheet thickness. Obtaining a sharp image of small structures is therefore dependent on creating a thin laser sheet.

The smallest possible perturbations in a turbulent flow are on the order of the Kolmogorov length scale η. This is the length over which turbulent kinetic energy can be dissipated by viscosity. Previous particle image velocimetry experiments and computational investigations of the current flowpath[5] have yielded estimates for the integral length scale L = 5 mm, root-mean square velocity u = 50 m/s, and kinematic viscosity υ = 4 to 5 m^2/s. The Kolmogorov length scale can be estimated using Equation 1[6] at η = 7 to 8 µm. The smallest flame structures are expected to be around ten times larger than the Kolmogorov length scale.[7] Therefore, a PLIF system that has both planar resolution and laser sheet thickness smaller than 70 µm should be able to observe the smallest flame structures in the flow.

$$\eta = (\upsilon/u)^{3/4} L^{1/4} \qquad (1)$$

Set-up

A long-duration visible light image of the cavity-stabilized flame is shown in Figure 1; the coordinate system shown originates in the plane of the backward-facing step at the downstream projection of the center of the nozzle exit. One wall had a copper insert with a cavity of step height H = 9 mm. Two side walls of the test section had quartz windows for camera access. The wall opposite the cavity had a quartz window for laser sheet insertion.

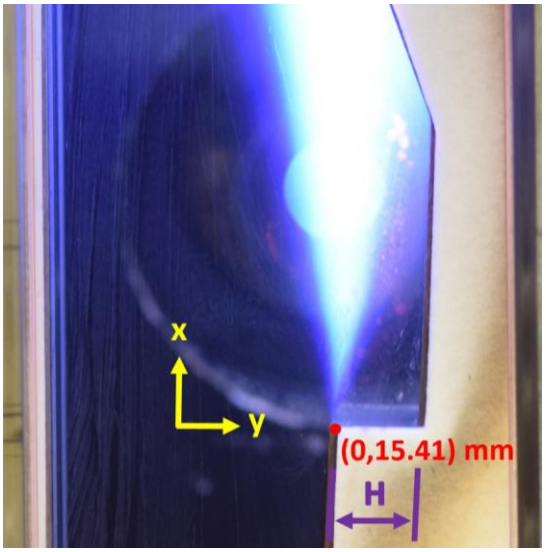

Figure 1: Cavity-anchored flame.

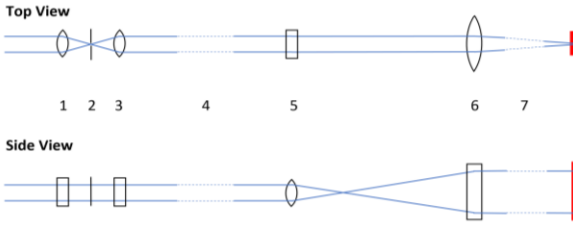

1. 500 mm focal length cylindrical lens
2. Spatial filter
3. 500 mm focal length cylindrical lens
4. Relay mirrors
5. 50 mm (200 mm) focal length cylindrical lens
6. 300 mm focal length spherical lens
7. planar mirror periscope
8. flame

Figure 2. OH (CH_2O) PLIF optics. *Not to scale.*

The PLIF beam path is described in Figure 2. A Q-switched Spectra-Physics Nd:YAG laser created a 1064 nm beam at 20 Hz. After frequency-doubling, the 532 nm beam pumped a Sirah Cobra-Stretch dye laser. For OH PLIF, the frequency-doubled dye laser output was tuned to 283.5525 nm, to excite the temperature-independent[3,8] $Q_1(8)$ transition of OH. The width of the laser sheet was decreased by a spatial filter (which was created using the entrance slit for a spectrometer) in which the gap between the

blunt sides of two steel blades was set by an adjustable knob. By narrowing the gap around the beam focus, the broad wings of the laser sheet were removed. The thickness of the OH PLIF laser sheet waist was measured using a 2448 x 2048 pixel, 16-bit CCD Point Grey beam-profiling camera (with the ultraviolet filter removed.) The laser sheet had full width at half-maximum of approximately 25 μm. Figure 3 shows profiles of laser sheet intensity at different spatial filter settings. The 125 μm setting was used for this data; smaller values caused slow ablation of the spatial filter.

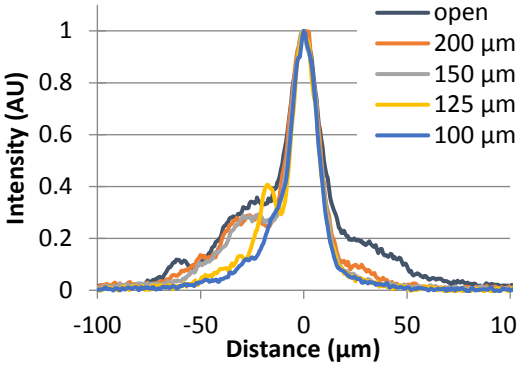

Figure 3. Effect of spatial filter setting on laser sheet intensity profile. *Settings are not absolute aperture widths; they are offset by an unknown constant value.*

PLIF images were taken using a PI-Max 4 intensified CCD camera with a square 13.1 mm sensor. OH PLIF images were taken with a 100 mm focal length, *f*/2.8 Cerco camera lens, with extension tubes and a Semrock FF02-320/40-30-D filter (bandpass from 310 to 340 nm) to block laser reflection and other interferences. The camera setup for OH PLIF was characterized using a USAF-1951 resolution target, shown in Figure 4. The target was backlit with an ultraviolet light source and images were taken using three extension tube lengths: 76.2, 152.4, and 203.2 mm.

For each line pair, a modulation value *m* was calculated according to Equation 2, using the maximum and minimum intensities *I* for the line pair. These "image" modulations were compared with a baseline "object" modulation measured at the large bright square and the adjacent dark area to calculate the modulation transfer function, *MTF*,[9] according to Equation 3. The resolution limit *RL* of the system was defined as the line pair width at which *MTF* = 50%.

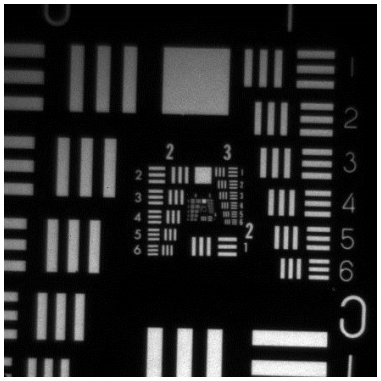

Figure 4. USAF-1951 resolution target. *Image taken with 76.2 mm extension tube configuration.*

$$m = \frac{I_{max} - I_{min}}{I_{max} + I_{min}} \quad (2)$$

$$MTF = \frac{m_{image}}{m_{object}} \quad (3)$$

For each extension tube length tested, image magnification *M* was recorded and compared with the resolution limit and the maximum signal intensity $I_{max,object}$. The product of resolution limit and magnification was approximately constant (Equation 4). As shown in Figure 5, signal intensity decreased with increasing magnification, consistent with Equation 5.[10]

$$RL \cdot M = 77\ \mu\text{m} \quad (4)$$

$$I \propto (M+1)^{-2} \quad (5)$$

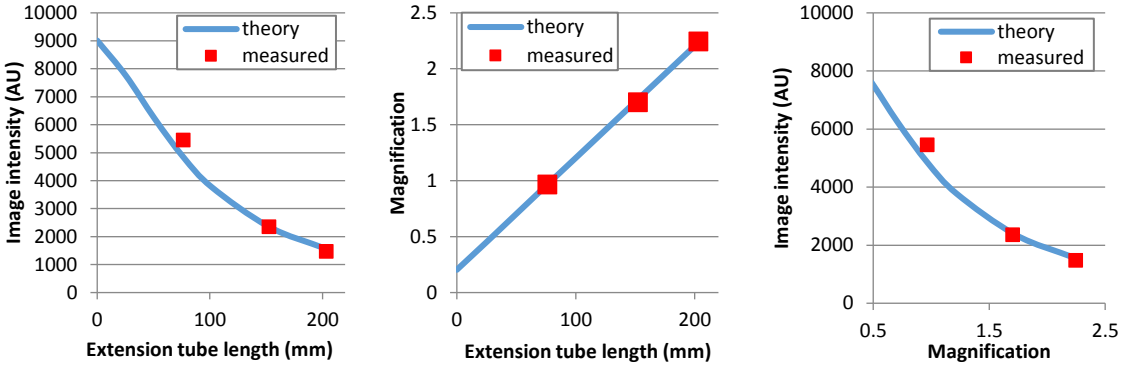

Figure 5. Magnification and image intensity values at different extension tube lengths.

The final system had magnification 1.91, corresponding to a field-of-view 6.86 x 6.86 mm across 512 x 512 pixels (or 13.4 μm/pixel) after 2 x 2 binning. The in-plane resolution was about 39 μm, based on a contrast transfer function of 50%. Three different motorized translation stages moved the sheet optics and the camera together to image different areas of the flow. Relay mirrors were used such that the laser sheet focus did not change during translation. A fourth motorized translation stage was used to move the camera towards or away from the laser sheet, adjusting the focus.

For CH_2O PLIF, laser output was tuned to 352.484 nm, using the $\tilde{A}^1A_2 - \tilde{X}^1A_1 4_0^1$ transition system commonly used to excite CH_2O.[11] Compared to the OH PLIF experiment, changes were made to the optical setup to promote a higher signal-to-noise ratio. The focal length of the cylindrical lens in the sheet optics (Element 5 in Figure 2) was increased to 200 mm, increasing laser sheet intensity by a factor of four. The camera was fitted with a visible light *f*/2 lens. The system had magnification 2.14, corresponding to a field-of-view 6.11 x 6.11 mm across 256 x 256 pixels (or 23.9 μm/pixel) after 4 x 4 binning. The camera used a GG-395 Schott filter to block laser reflection.

Methods and data processing

To investigate a large area, images were taken while the translation system's *x*-axis motor was in motion. Camera focus was periodically adjusted. Background image sets were acquired with the laser blocked. Mean background images have been subtracted from all presented results.

For OH PLIF, the camera travelled along the *x*-axis at 0.25 mm/s while acquiring images at 10 Hz, resulting in 40 images for every millimeter. Six *x*-direction sweeps were acquired from x/H = 0 to 14.10, and from y/H = -0.67 to 2.70.

CH_2O PLIF images were captured at 20 Hz while the camera travelled at 0.5 mm/s. Five *x*-direction sweeps were captured from x/H = 0 to 14.01, and from y/H = -0.52 to 2.05. Imaging was attempted closer to the cavity wall, but the ablation of the wall by the laser created bright interference that obscured flame structure in many images.

Results and discussion

For OH PLIF, Figure 6 shows selected single shot images, while Figure 7 shows a compilation of single shots across the test

section. In these images, OH signal marks the location of combustion products in the flow. The edge of the signal is the interface between reactants and products. This marks the general location of the flame front.[12] The images show evidence of flamelets,[13] where reactants and products are separated by wrinkled flames on the order of 100 μm wide.

Intermittency was calculated across the test section. For a given pixel location, intermittency is defined as the fraction of images in which significant OH signal is detected.[3] Figure 8 shows flame boundaries with 10% and 90% intermittency. This gives a visualization of the region in which the flame front oscillates.

The images were analyzed for the smallest flame structures in the flow. Figure 9 shows an OH PLIF intensity profile (at the yellow line) across a small flame structure (in the lower right quadrant of the first image in Figure 6.) It has a full width at half-maximum of approximately 110 μm, and is representative of the smallest structures

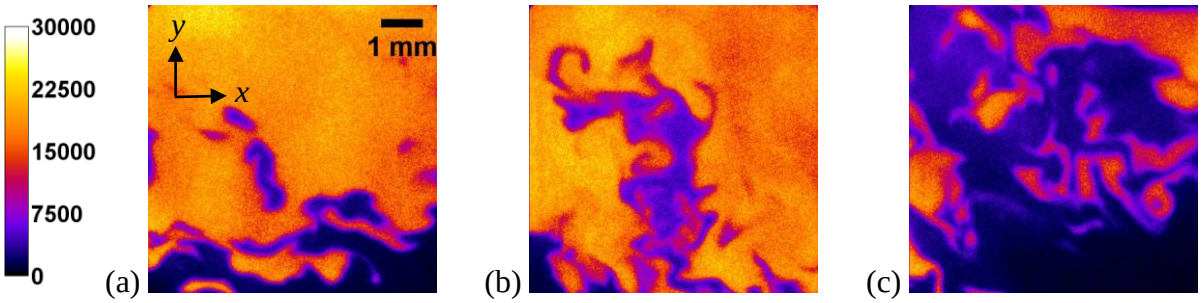

Figure 6. Selected OH PLIF images. *False color. Downstream of the cavity. Image center coordinates:* x/H = *(a) 5.60, (b) 5.65, (c) 6.25,* y/H = *1.60.*

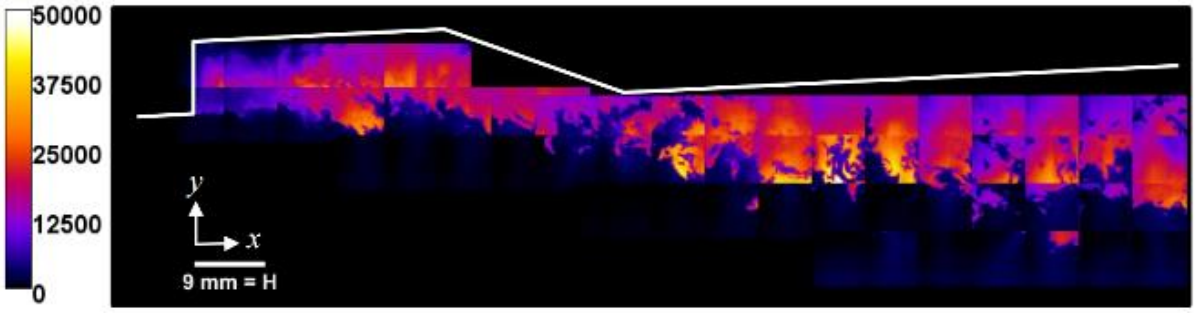

Figure 7. Compilation of OH PLIF images across the test section. *False color.*

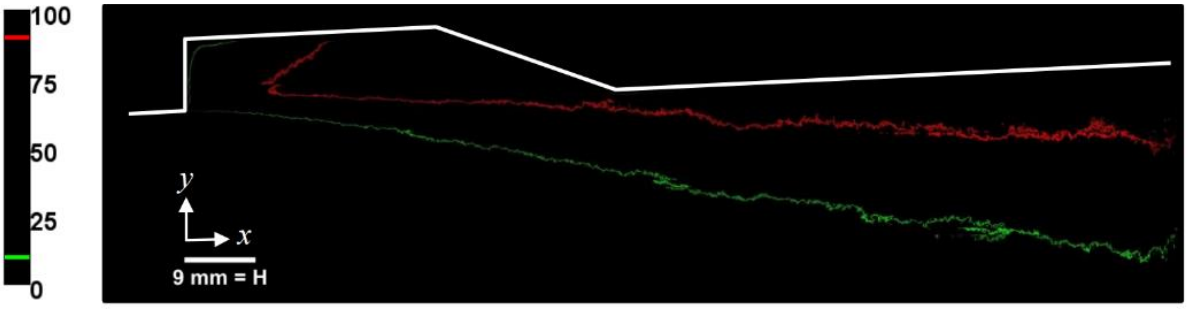

Figure 8. OH PLIF intermittency boundaries. *Based on threshold signal intensity 6,000 counts.*

observed. This is slightly larger than the predicted size for the smallest flame structures (70 – 80 μm.) No structures near the predicted resolution of the system (39 μm) were observed. This suggests that this OH PLIF system is capable of resolving all flame structure length scales for this turbulent compressible flowfield.

For CH_2O PLIF, selected single shots are presented in Figure 10. CH_2O signal marks the preheat zone of the flame,[12] which in some locations is significantly wider than the flame thickness. The smallest observed CH_2O were larger than the smallest OH features, approximately 200 μm wide. This may be due to significantly decreased signal intensity as well as decreased spatial resolution caused by increased pixel binning. CH_2O PLIF images suffered from a much smaller signal-to-noise ratio than OH PLIF. CH_2O PLIF images were also frequently marred by bright interference created by the laser sheet ablating the copper wall.

Conclusions

This work has demonstrated an OH PLIF system that can resolve premixed turbulent flame structures in a high-speed compressible reacting flow as small as 25 x 40 x 40 μm^3. However, the observed CH_2O PLIF signal was much weaker than the OH PLIF signal, resulting in decreased resolution. Work is ongoing to improve these issues with high-resolution CH_2O PLIF.

Next steps

Preliminary CH_2O PLIF imaging was performed on a simple propane flame using excitation wavelengths near 338 nm. Compared with 352.5 nm excitation, signal

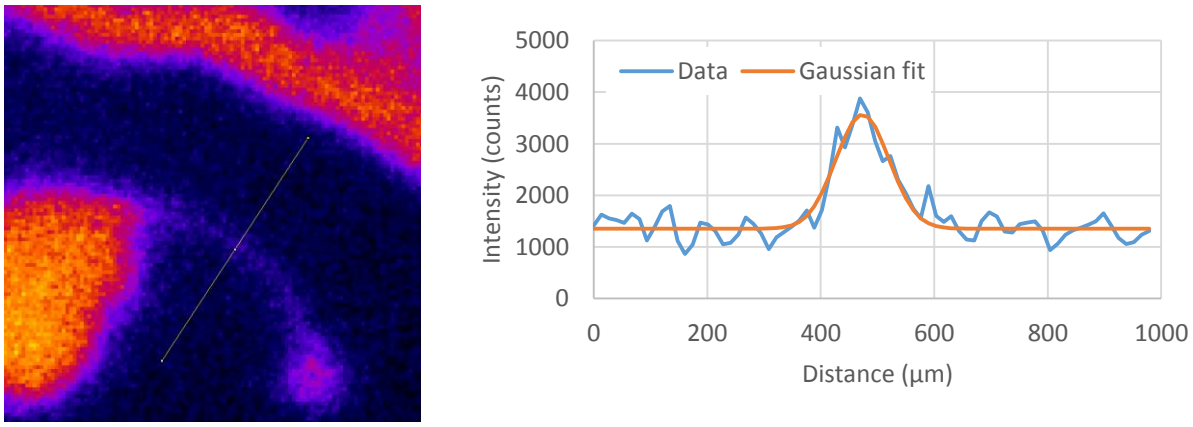

Figure 9. OH PLIF small structure profile.

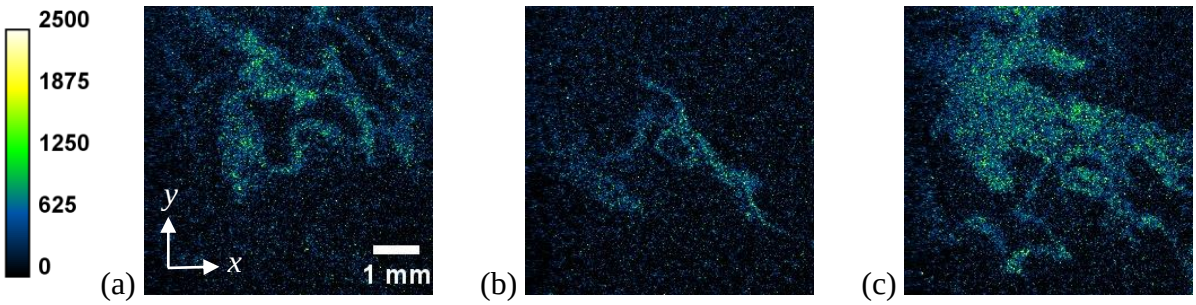

Figure 10. Selected CH_2O PLIF images. *False color. In the mixing region adjacent to the cavity. Image center coordinates:* x/H = *(a) 4.61, (b) 4.73, (c) 4.86,* y/H = *1.71.*

was improved nearly twofold. Paul and Najm also report significantly better signal at this band.[12] Using this band may increase PLIF signal during the next facility test. Other possible measures to improve signal include switching to an *f*/1.2 camera lens, decreasing image magnification, and lowering the lens filter cutoff wavelength. Increasing the focal length of the sheet-forming cylindrical lens (Element 5 in Figure 2) would decrease the height of the sheet and increase its energy density; this may also increase PLIF signal.

These high-resolution PLIF techniques will be used in the near future to validate and investigate an entirely new scramjet combustor geometry (Figure 11), currently in the design process. The design for the new insert is modular and relies on additive manufacturing with Inconel 718. This means that new geometries can be printed on-demand and tested in the facility with relative ease.

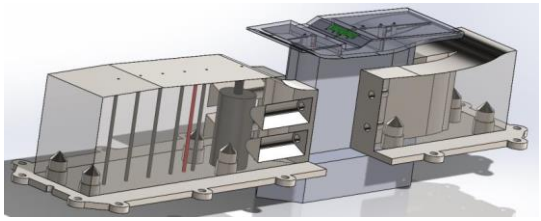

Figure 11. Modular scramjet insert design.

Acknowledgements

The author would like to thank his advisor, Dr. Harsha Chelliah, as well as Dr. Andrew Cutler, Dr. Paul Danehy, Dr. Robert Rockwell, Christopher Spelker, and Zeid Hashem for their work on this project. The help of Damien Lieber, Justin Kirik, Dr. Chris Goyne, and Dr. Ross Burns was very much appreciated.

The author is very grateful for the support of the Virginia Space Grant Consortium Graduate Research Fellowship Program. This research is also funded by the National Science Foundation award #1511520 (program officer Dr. Song-Charng Kong) and the Air Force Office of Scientific Research award #FA9550-15-0440 (technical monitor Dr. Chiping Li.)

Literature Cited

[1] R. D. Rockwell, C. P. Goyne, B. Rice, H. K. Chelliah, J. C. McDaniel, J. R. Edwards, L. Cantu, E. Gallo, A. D. Cutler, P. M. Danehy, Development of a Premixed Combustion Capability for Dual-Mode Scramjet Experiments, 53rd AIAA Aerospace Sciences Meeting (2015.)

[2] K. N. Gabet, R. A. Patton, N. Jiang, W. R. Lempert, J. A. Sutton, High-speed CH_2O PLIF imaging in turbulent flames using a pulse-burst laser system, Appl. Phys. B 106 (2012) 569-575.

[3] L. M. L. Cantu, E. C. A. Gallo, A. D. Cutler, P. M. Danehy, R. D. Rockwell, C. T. Johansen, C. P. Goyne, J. C. McDaniel, OH PLIF Visualization of a Premixed Ethylene-fueled Dual-Mode Scramjet Combustor, 54th AIAA Aerospace Sciences Meeting (2016.)

[4] P. M. Allison, K. Frederickson, W. R. Lempert, J. A. Sutton, J. W. Kirik, R. D. Rockwell, C. P. Goyne, Investigation of Flame Structure and Combustion Dynamics using CH_2O PLIF and High-Speed CH* Chemiluminescence in a Premixed Dual-Mode Scramjet Combustor, 54th AIAA Aerospace Sciences Meeting (2016.)

[5] K. Ramesh, J. R. Edwards, C. P. Goyne, J. C. McDaniel, A. D. Cutler, P. M. Danehy, Large Eddy Simulation of High-Speed,

Premixed Ethylene Combustion, 53rd AIAA Aerospace Sciences Meeting (2015.)

[6] J. Westerweel, G. E. Elsinga, R. J. Adrian, Particle Image Velocimetry for Complex and Turbulent Flows, Annual Rev. Fluid Mechanics 45 (2013) 409-436.

[7] H. Kobayashi, T. Kawahata, K. Seyama, T. Fujimari, J. Kim, Relationship between the smallest scale of flame wrinkles and turbulence characteristics of high-pressure, high temperature turbulent premixed flames, Proc. Combust. Inst. 29 (2002) 1793-1800.

[8] S. O'Byrne, I. Stotz, A. Neely, R. Boyce, N. Mudford, F. Houwing, OH PLIF Imaging of Supersonic Combustion Using Cavity Injection, AIAA/CIRA 13th International Space Planes and Hypersonics Systems and Technologies Conference (2005.)

[9] W. J. Smith, Modern optical engineering: the design of optical systems, McGraw Hill, New York, 2000, pp. 366-372.

[10] N. T. Clemens, Flow Imaging, in: J. P. Hornak (Ed.), Encyclopedia of Imaging Science and Technology. Wiley, New York, 2002, pp. 390-419

[11] B. O. Ayoola, R. Balachandran, J. H. Frank, E. Mastorakos, C. F. Kaminski, Spatially resolved heat release rate measurements in turbulent premixed flames, Combust. Flame 144 (2006) 1-16.

[12] P. H. Paul, H. N. Najm, Planar Laser-Induced Fluorescence Imaging of Flame Heat Release Rate, Symp. (Int.) Combust. 27 (1998) 43-50.

[13] J. F. Driscoll, Turbulent premixed combustion: Flamelet structure and its effect on turbulent burning velocities, Prog. Energy Combust. Science 34 (2008) 91-134.